

## Article

# Analysis of Selected Dielectric Properties of Epoxy-Alumina Nanocomposites Cured at Stepwise Increasing Temperatures

Anna Dąda <sup>1</sup>, Paweł Błaż <sup>1,\*</sup>, Maciej Kuniewski <sup>2</sup> and Paweł Zydrón <sup>2,\*</sup>

<sup>1</sup> AGH Doctoral School, AGH University of Science and Technology, Al. Mickiewicza 30, 30-059 Kraków, Poland

<sup>2</sup> Department of Electrical and Power Engineering, Faculty of Electrical Engineering, Automatics, Computer Science, and Biomedical Engineering, AGH University of Science and Technology, Al. Mickiewicza 30, 30-059 Kraków, Poland

\* Correspondence: pblaut@agh.edu.pl (P.B.); pzydron@agh.edu.pl (P.Z.)

**Abstract:** The paper presents the effects of gradual temperature curing on the dielectric properties of epoxy nanocomposite samples. Samples were prepared based on Class H epoxy resin filled with nano-alumina (Al<sub>2</sub>O<sub>3</sub>) for different wt% loadings (0.5 wt% to 5.0 wt%) and two different filler sizes (13 nm and <50 nm), i.e., two different specific surface area values. During the research, specimen sets were cured gradually at increasingly higher temperatures (from 60 °C to 180 °C). Broadband dielectric spectroscopy (BDS) was used to determine the characteristics of the dielectric constant and the dielectric loss factor in the frequency range from 10<sup>-3</sup> Hz to 10<sup>5</sup> Hz. As a result, it was possible to analyze the impact of the progressing polymer structure thermosetting processes on the observed dielectric parameters of the samples. The nano-Al<sub>2</sub>O<sub>3</sub> addition with 0.5 wt%, 1.0 wt%, and 3.0 wt% resulted in a decrease in dielectric constant values compared to neat epoxy resin samples. The most significant reductions were recorded for samples filled with 0.5 wt% of 13 nm and <50 nm powders, by about 15% and 11%, respectively. For all tested samples, the curing process at a gradually higher temperature caused a slight decrease in the dielectric constant (approx. 2% to 9%) in the whole frequency range. Depending on the nanofiller content and the curing stage, the dielectric loss factor of the nanocomposite may be lower or higher than that of the neat resin. For all tested samples cured at 130 °C (and post-cured at 180 °C), the differences in the dielectric loss factor characteristics for frequencies greater than 100 Hz are low. For frequencies < 100 Hz, there are prominent differences in the characteristics related to the size of the nanoparticle and the individual wt% value. At a small nanofiller amount (0.5 wt%), a decrease in the dielectric constant and dielectric loss factor was observed for frequencies < 100 Hz for samples with nanofillers of both sizes.

**Keywords:** electrical insulation; nanodielectrics; nanocomposites; epoxy resin; nanofiller; alumina; dielectric constant; dielectric loss factor; BDS



**Citation:** Dąda, A.; Błaż, P.; Kuniewski, M.; Zydrón, P. Analysis of Selected Dielectric Properties of Epoxy-Alumina Nanocomposites Cured at Stepwise Increasing Temperatures. *Energies* **2023**, *16*, 2091. <https://doi.org/10.3390/en16052091>

Academic Editor: Dumitran Laurentiu

Received: 24 November 2022

Revised: 16 February 2023

Accepted: 17 February 2023

Published: 21 February 2023



**Copyright:** © 2023 by the authors. Licensee MDPI, Basel, Switzerland. This article is an open access article distributed under the terms and conditions of the Creative Commons Attribution (CC BY) license (<https://creativecommons.org/licenses/by/4.0/>).

## 1. Introduction

The constantly growing demand for high-quality electricity requires increasing the reliability of its supply through transmission and distribution networks. Such a course makes it necessary to improve the design and construction of used electrical equipment and installations. That task is carried out in particular through intensive research in terms of insulating materials technology. One of the development paths with high application potential in this field is nanocomposites use. Experimental research verifying their features is needed because the nanofiller influence on the composite material properties is not always apparent. The development of new insulating materials and the modification of the properties of existing ones using modern materials engineering methods is a response to the ever-increasing technical requirements for electrical insulating systems. Such an approach particularly applies to materials used in high-voltage applications [1–3]. These requirements result, first of all, from the gradual increase in the rated power and operating voltage levels

of electrical devices and networks, as well as the required increase in their reliability and extension of their technical service life. One of the most promising research directions that could help to obtain materials with significantly improved dielectric properties is the intentional, controlled modification of high-molecular polymer structures of dielectrics with nanoparticle fillers of different types [1–13]. Many studies also concern obtaining such modifications of the structures and properties of polymer nanocomposites that will increase their thermal conductivity. The functional purpose of these changes is to improve cooling conditions and heat dissipation in working electric devices and machines [14–17].

The idea of using polymer nanocomposites as new, specific materials for electrical insulation was presented by T. J. Lewis in 1994 [18], and to the present day, there is a significant and very fast-rising number of research, publications, and patents in this area. The continuously growing interest in nanocomposites is related to their properties (and the possibility of their effective control), which in many cases are much more advantageous compared to polymers without fillers or modified with microfillers [1,3,19].

The addition of small, by weight or volume, amounts of nanometric inorganic particles to the structures of various polymer types (polyolefins, epoxies, etc.) enables the creation of new, modified materials with high potential for many electrical applications. The most important advantages of nanocomposites include noticeably better mechanical, thermal, and electrical properties, and the synergy of improving these parameters is also observed in many cases. The modification of dielectric properties in nanocomposites is related to their high interphase, the volume effect of which increases with the reduction of nanofiller particle size. Nanofillers have the potential to develop strong interfacial interactions between the structure of the base polymer material and nanoparticles due to their very large specific surface area. This effect is more noticeable when the size of the nanoparticles is smaller. Interphase can cause a change in the chemical composition, at the same time affecting the mobility of the polymer chain, the degree of hardening, or the crystallinity of the resin [20].

The properties of the nanocomposite, its structure, and morphology are influenced by the components (base polymer material and nanofiller), as well as the method and procedure of its manufacture. Any inhomogeneities resulting from the imperfect mixing of the nanofiller with the base, the ingress of contaminants or water, and the occurrence of internal defects, e.g., gaseous inclusions, may lead to distortion of the measurement results and misinterpretation of changes in dielectric properties caused by the presence of nanofillers in the composite structure [13,17,19,21].

Epoxy resins are often used as the base material of nanocomposites, which due to their good mechanical and electrical strength parameters, as well as the ease of forming the required shape, are commonly used in the production of many electrical devices. Resins are one of the most versatile insulating materials used in insulators, spacers, bushings, current transformers (CT), voltage transformers (VT), generators, motors, PCBs, and others [4,22–25].

One of the most commonly used nanofillers are nanoparticles of oxide compounds, such as  $\text{Al}_2\text{O}_3$ ,  $\text{TiO}_2$ , and  $\text{SiO}_2$ . They are indicated as one of the most advantageous admixtures due to their excellent mechanical properties (stiffness, strength, and hardness), chemical inertness (resistance to oxidation and corrosion processes), thermal stability at very high temperatures, and relatively low cost compared to other nanofillers, e.g., carbon nanotubes [1,22,26–28].

This paper presents the results of research on nanocomposite samples made based on epoxy resin modified with nano-particles of aluminum oxide ( $\text{Al}_2\text{O}_3$ ), with two different sizes of nanofiller (13 nm and 50 nm). Alumina is relatively often used as a nanofiller also in the research work of other teams, which focused on the analysis of the dielectric properties of such composites and their applications [29–38]. The program of the described research is partly related to the previously published research [39], but it also provides for the influence of thermal processing (pre- and post-curing) on the stabilization of the dielectric properties of epoxy-based nanocomposites. The purpose of this study is to fill a certain gap in this area.

After the manufacture of nanocomposite specimens, they were subjected to pre-curing, curing, and post-curing processes in three consecutive thermal test cycles. Each cycle was run for 8 h at stabilized temperatures (60 °C, 130 °C, or 180 °C). Then, in each cycle, the composite samples were cooled to ambient temperature (23 °C), and then the dielectric constant and the dielectric loss factor were measured in a wide frequency range. In this way, it was monitored how the gradually progressing cross-linking process of the base epoxy resin affects the dielectric parameters of the nanocomposite samples. The comparison of the results makes it possible to evaluate the character of observed changes after each thermal curing cycle.

## 2. Experiment Description

### 2.1. Materials for Tested Samples

The research concerned samples of nanocomposite materials based on epoxy resin and alumina nanofillers with two different sizes of nanoparticles, which were added to the resin with a controlled weight percentage (wt%). The Epoxylite<sup>®</sup> 235SG resin (supplied by Elantas) [40] was used as a base material for the production of specimens. It is an epoxy resin based on diglycidyl ether of bisphenol-A (DGEBA) as a main component cured with an aliphatic amine-based hardener. These types of resins have been widely used in the electrical industry for many decades; therefore, their properties have been thoroughly studied [41–46]. The product is intended for use in electrical insulating systems with maximum temperature ratings of class H (180 °C). According to the information provided by the manufacturer, the main applications of this resin are trickle impregnation and sealing of rotor and stator windings. The high chemical resistance of this resin ensures long-term operation in all hermetic applications [40].

Aluminum oxide Al<sub>2</sub>O<sub>3</sub> nanopowders supplied by Sigma-Aldrich were used as fillers [47,48]. Alumina is a widely available metal oxide that has been used for a long time in various industrial applications, and almost from the beginning of research on nanodielectrics as a nanofiller in polymer composites [36–38]. For comprehensive, nanoparticle size-dependent analysis, the test samples were prepared using two nanopowders with significantly different average sizes of <50 nm and 13 nm. For the epoxy resin used to make the specimens and for both average particle sizes, the parameters characteristic for the produced nanocomposites were estimated, assuming that nanofiller particles are homogeneously arranged in a whole specimen volume as a simple cubic lattice:

(1) Inter-particle distance  $D$ , defined as the smallest distance between evenly distributed nanofiller particles [49,50]:

$$D = \left\langle \left\{ \frac{\pi}{6} \left( \frac{\rho_n}{\rho_m} \right) \frac{100\%}{wt\%} \left[ 1 - \frac{wt\%}{100} \left( 1 - \frac{\rho_m}{\rho_n} \right) \right] \right\}^{\frac{1}{3}} - 1 \right\rangle d \quad (1)$$

(2) Relative distance ( $RD$ ), which we define as the ratio of the inter-particle distance  $D$  to the average size of the nanoparticle  $d$ :

$$RD = D/d \quad (2)$$

(3) Filler surface area ( $FSA$ ) [48,49]:

$$FSA = \frac{\pi d^2}{(D+d)^3} = \pi \left( \frac{d}{D+d} \right)^2 \frac{1}{D+d} \quad (3)$$

where:

$d$ —nanofiller particle average diameter [m];

$D$ —inter-particle distance [m];

$FSA$ —nanofiller surface area per unit volume [m<sup>2</sup>/m<sup>3</sup>];

$\rho_n$ —specific density for nanofiller [kg/m<sup>3</sup>];

$\rho_m$ —specific density for polymer matrix [kg/m<sup>3</sup>];

EpoxyLite 235SG (resin + hardener):  $\rho_m = 1.13 \text{ g/cm}^3$ ;

Alumina  $\text{Al}_2\text{O}_3$  nanopowder:  $\rho_n = 4.000 \text{ g/cm}^3$ .

Estimation results of the above-mentioned parameters for the tested composite materials are presented in Table 1.

**Table 1.** Selected parameters describing tested composite materials.

| Filler Content wt%<br>(%)                                | Inter-Particle Distance<br>(nm) | Relative Distance<br>(1) | FSA<br>( $\text{km}^2/\text{m}^3$ ) |
|--|---------------------------------|--------------------------|-------------------------------------|
| $\text{Al}_2\text{O}_3$<br>nanoparticle dimension 13 nm  |                                 |                          |                                     |
| 0.5  | 80.3                            | 6.17                     | 0.654                               |
| 1  | 60.9                            | 4.69                     | 1.313                               |
| 3  | 38.0                            | 2.92                     | 3.998                               |
| 5  | 29.8                            | 2.29                     | 6.762                               |
| $\text{Al}_2\text{O}_3$<br>nanoparticle dimension <50 nm |                                 |                          |                                     |
| 0.5  | <308.7                          | 6.17                     | >0.170                              |
| 1  | <234.4                          | 4.69                     | >0.341                              |
| 3  | <146.2                          | 2.92                     | >1.039                              |
| 5  | <114.7                          | 2.29                     | >1.758                              |

Both the inter-particle distance  $D$  and the  $FSA$  of the filler nanoparticles depend on the value of wt% and the nanoparticle average diameter  $d$ . For a higher value of wt%, the distance  $D$  is smaller and the value of  $FSA$  is greater. For a smaller nanoparticle size, the distance  $D$  decreases while the  $FSA$  increases. It should be noted that the relative distance of the nanoparticles (described by  $RD$  parameter) is dependent on wt%, but independent of their average diameter  $d$ , i.e., it is the same for different sizes of nanoparticles. This parameter depends only on the values of wt%,  $\rho_m$ , and  $\rho_n$ .

## 2.2. Preparation of Samples

The method of preparation and pre-treatment of used components as well as the sample preparation procedure has a major impact on the subsequent properties of the obtained nanocomposites. Many factors can affect the specimen formation process. The key issue is the correct dispersion of the nanofiller particles in the base material and the appropriate low level of moisture of the individual components. The samples were manufactured by the direct mixing method [35], based on procedures described in the literature [21,23,26,27] and practical laboratory experience.

The procedure for the manufacturing of material samples in laboratory conditions was carried out in several stages, with a strict, repeatable time and temperature regime. First, the nanofiller was dried with a moisture analyzer. Each admixture was dried at  $160 \text{ }^\circ\text{C}$  for a time sufficient to achieve a stable weight of the nanopowder, indicating that its water content was removed. Then, the proper weight proportions of individual reagents (epoxy resin, hardener, nanofiller) were determined.

The next step was to mix the ingredients. A mechanical mixer was used for this purpose. Duration and intensity of mixing depended on the consistency of the mix at different wt% of added nanofiller. Due to the gelation time of the EpoxyLite 235SG resin declared by the manufacturer (35 min) [40], resin and nanofiller were mixed first. After the hardener had been added, mixing was continued for a few more minutes before proceeding to the next sample manufacturing operation.

Degassing the epoxy resin with a nanofiller to remove gaseous inclusions is an essential and demanding step for the proper preparation of the sample. Possible gaseous inclusions can influence the dielectric parameters of the nanocomposite, reduce the dielectric strength,

and be the source of partial discharges. The degassing process of the epoxy nano-mixture prepared for the production of test samples was carried out in a vacuum chamber with a controlled pressure of 50 hPa. Dosing of the prepared, liquid mixture into the molds was also carried out under vacuum conditions. After pouring, the specimens were allowed to pre-cure at a pressure of about 500 hPa and a temperature of 30 °C for 24 h. The finished, solidified specimens were stored in a dry, dark place at ambient temperature (21 °C to 23 °C).

For the described tests, nine specified sets of samples with dimensions of 100 mm × 100 mm × 1 mm were made, no fewer than three samples in each set. The size of the specimens was fitted to the size of the measuring three-electrode air capacitor used in the measuring stand. The summary of all the specimens' sets is presented in Table 2.

**Table 2.** Individual sets of the tested epoxy/alumina specimens.

| Specimens Set No. | Nanoparticle Size | Specimen Composition                                   |
|-------------------|-------------------|--|
| 1                 | -                 | Neat epoxy resin                                       |
| 2                 | 13 nm             | epoxy resin + 0.5% Al <sub>2</sub> O <sub>3</sub> (wt) |
| 3                 | 13 nm             | epoxy resin + 1.0% Al <sub>2</sub> O <sub>3</sub> (wt) |
| 4                 | 13 nm             | epoxy resin + 3.0% Al <sub>2</sub> O <sub>3</sub> (wt) |
| 5                 | 13 nm             | epoxy resin + 5.0% Al <sub>2</sub> O <sub>3</sub> (wt) |
| 6                 | 50 nm             | epoxy resin + 0.5% Al <sub>2</sub> O <sub>3</sub> (wt) |
| 7                 | 50 nm             | epoxy resin + 1.0% Al <sub>2</sub> O <sub>3</sub> (wt) |
| 8                 | 50 nm             | epoxy resin + 3.0% Al <sub>2</sub> O <sub>3</sub> (wt) |
| 9                 | 50 nm             | epoxy resin + 5.0% Al <sub>2</sub> O <sub>3</sub> (wt) |

### 2.3. Experimental Setup and Measuring Instruments

One of the universal research methods used to study the parameters of insulating materials is broadband dielectric spectroscopy, BDS [51,52]. This method enables obtaining a range of detailed dielectric information about the tested material. The basic parameters that can be obtained are the spectra of the dielectric constant  $\epsilon_r$  and the dielectric loss factor  $\tan\delta$ . These dielectric parameters of the tested materials are calculated based on the results of impedance measurements, taking into account the individual geometric dimensions of the tested samples [51].

The measuring stand was equipped with a supervising computer, a Solartron 1260A Impedance/Gain-Phase Analyzer (high-precision frequency response analyzer, FRA) [53] with a Solartron 1296A Dielectric Interface [54], and a solid dielectric sample holder (adjustable, three-electrode air capacitor with a dial micrometer, for precise determination of the tested specimen thickness), see Figure 1a.

Sample holder used for broadband measurements has two disk electrodes, "High" (voltage electrode) and "Low" (current electrode), which are guarded by a ring electrode (Figure 1b), as recommended by IEC 62631-2-1 [55] and ASTM D150-18 [56]. All electrodes are made of stainless steel. The configuration and geometry of the three-electrode system, in which the solid dielectric sample is placed, allow to: (1) eliminate the influence of stray capacitance and surface current on the value of measured parameters and (2) reduce the undesirable edge effect, disturbing the uniform distribution of the electric field in the sample near the edge of the current electrode.

The joint use of these specialized measuring instruments allows the characteristics collection of the dielectric constant and the dielectric loss factor of the tested material samples over a wide frequency range, with very high accuracy. For this purpose, the dielectric parameters of the tested materials were calculated based on the impedance measurement results of the three-electrode capacitor (the real and imaginary parts of

complex relative permittivity were determined for each frequency). In the calculations for a particular tested sample, its individual geometric dimensions were taken into account.

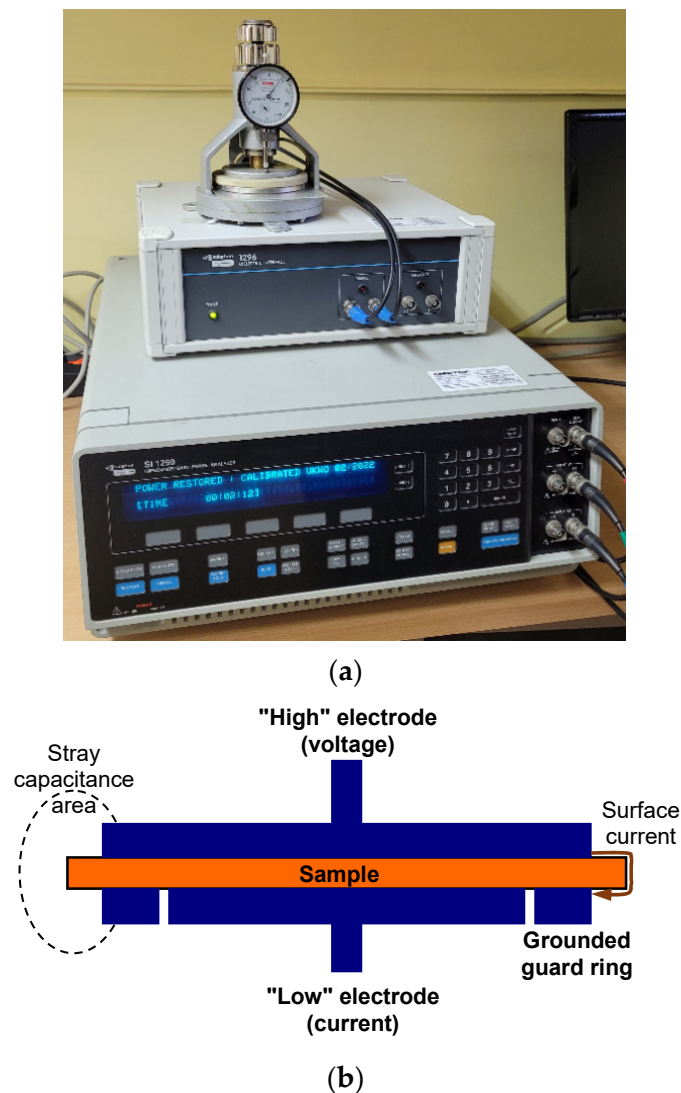


**Figure 1.** Broadband dielectric characteristics measurement setup: (a) test stand with Solartron 1260A Frequency Response Analyzer [53], Solartron 1296A Dielectric Interface [54] and solid dielectric sample holder, adjustable three-electrode capacitor; (b) configuration of disk electrodes with guard-ring in the sample holder, as recommended in [55,56] for solid dielectric samples.

#### 2.4. Experiment Procedure

The research procedure was aimed at determining the effect of gradual temperature curing of nanocomposite samples on the broadband characteristics of the dielectric constant and the dielectric loss factor. Every specimen set was tested in four consecutive cycles. For the first time, sample parameters were tested after their manufacture, when they were not exposed to a temperature other than the ambient one. Then, they were measured after pre-curing for 8 h at 60 °C in a vacuum oven. Next, two series of similar measurements were carried out after 8 h of thermal curing at 130 °C and post-curing at 180 °C, respectively. The temperatures were selected following the datasheet of the epoxy resin used. Class H insulation material's maximum allowed a hotspot temperature of 180 °C [57]. The measurements of the dielectric constant  $\epsilon_r$  and dielectric loss factor  $\tan\delta$  were performed at low voltage AC signal (2.0 V) in the wide frequency range, covering eight decades, from  $10^{-3}$  Hz to  $10^5$  Hz. They were performed at the end of each curing cycle after the samples

had cooled down and thermally stabilized at an ambient temperature of 23 °C. Acquired data were averaged for individual specimen sets and then analyzed and visualized as broadband dielectric parameter characteristics using the Matlab<sup>®</sup> software package (The MathWorks, Inc.). To ensure the possibility of comparing the characteristics of the analyzed dielectric parameters, all tested samples were visualized on the same scale, in the same range of values.

### 3. Results of Dielectric Parameters Measurement

The results of broadband measurements of the dielectric constant  $\epsilon_r$  and the dielectric loss factor  $\tan\delta$  of specimens from neat epoxy resin (without nanofillers) constituted the basic reference for the tests performed for the series of samples with  $\text{Al}_2\text{O}_3$  nanofiller. They are summarized for all sample curing temperatures in Figure 2.

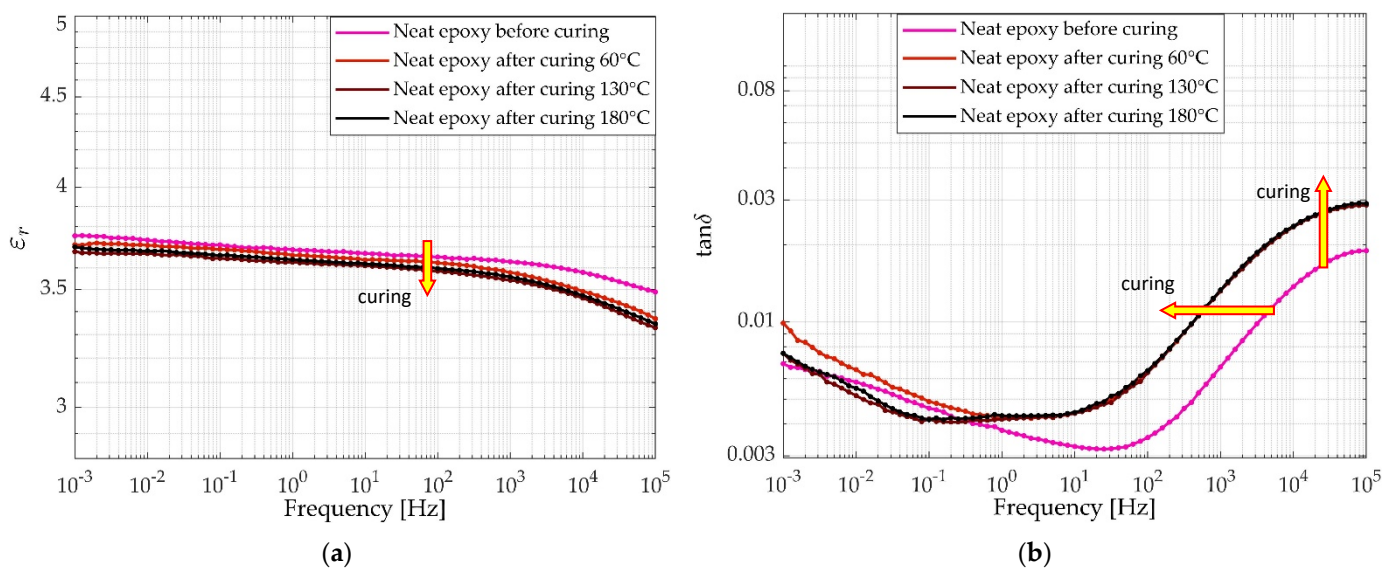


**Figure 2.** Broadband characteristics of dielectric constant  $\epsilon_r(f)$  (a) and dielectric loss factor  $\tan\delta(f)$  (b) for neat epoxy specimens before and after subsequent thermal curing cycles.

The results of dielectric constant measurements for composite samples (with nanofillers) were summarized in two groups, each of which was visualized in relation to one of two parameters, wt% or curing cycle temperature. Figures 3 and 4 present the characteristics of  $\epsilon_r(f)$  parameterized against wt% for the measurements made on new specimens and after subsequent cycles of their thermal curing, for the 13 nm and 50 nm  $\text{Al}_2\text{O}_3$  nanofiller, respectively. In turn, Figures 5 and 6 show the same characteristics but are parameterized with respect to the temperature of the thermal curing cycle for measurements made on specimens with different wt%, for the  $\text{Al}_2\text{O}_3$  nanofiller 13 nm and 50 nm, respectively. The method of presenting the data allows for detailed comparative analysis in both parameterized groups.

The results of the dielectric loss factor  $\tan\delta(f)$  measurements for composite samples (with nanofillers) were also summarized in two groups, each visualized in relation to a different parameter. Figures 7 and 8 present the characteristics of  $\tan\delta(f)$  parameterized against wt% for the measurements made on new specimens and after subsequent cycles of their thermal curing, for the 13 nm and <50 nm  $\text{Al}_2\text{O}_3$  nanofiller respectively. Next, Figures 9 and 10 show the same characteristics but are parameterized with respect to the temperature of the thermal curing cycle for measurements made on specimens with different wt% for the  $\text{Al}_2\text{O}_3$  nanofiller 13 nm or <50 nm, respectively.

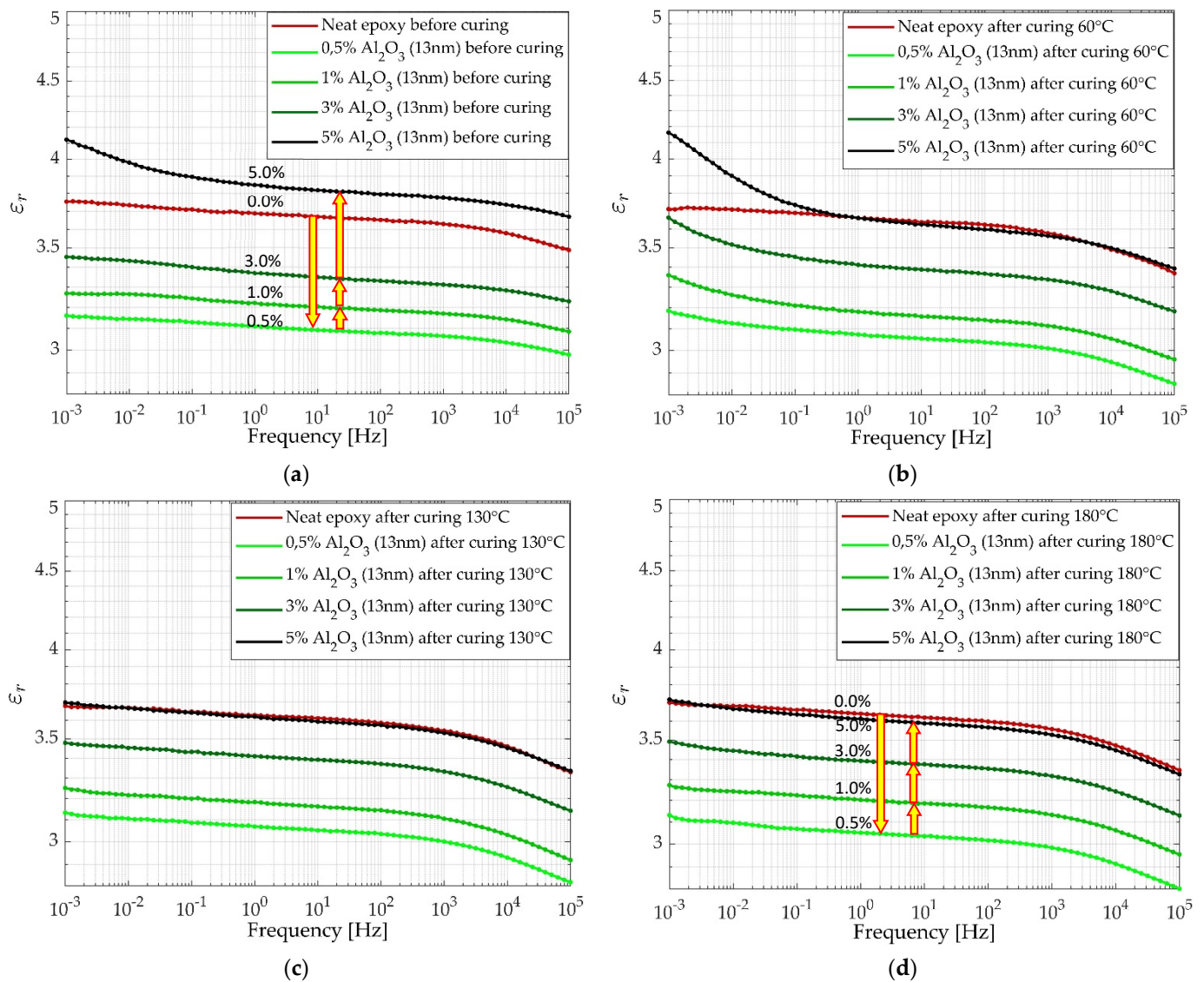


**Figure 3.** Broadband dielectric constant  $\epsilon_r(f)$  characteristics for samples with Al<sub>2</sub>O<sub>3</sub>, with particles of 13 nm: (a) new, before curing, (b) after thermal curing at 60 °C, (c) after thermal curing at 130 °C, (d) after thermal curing at 180 °C.

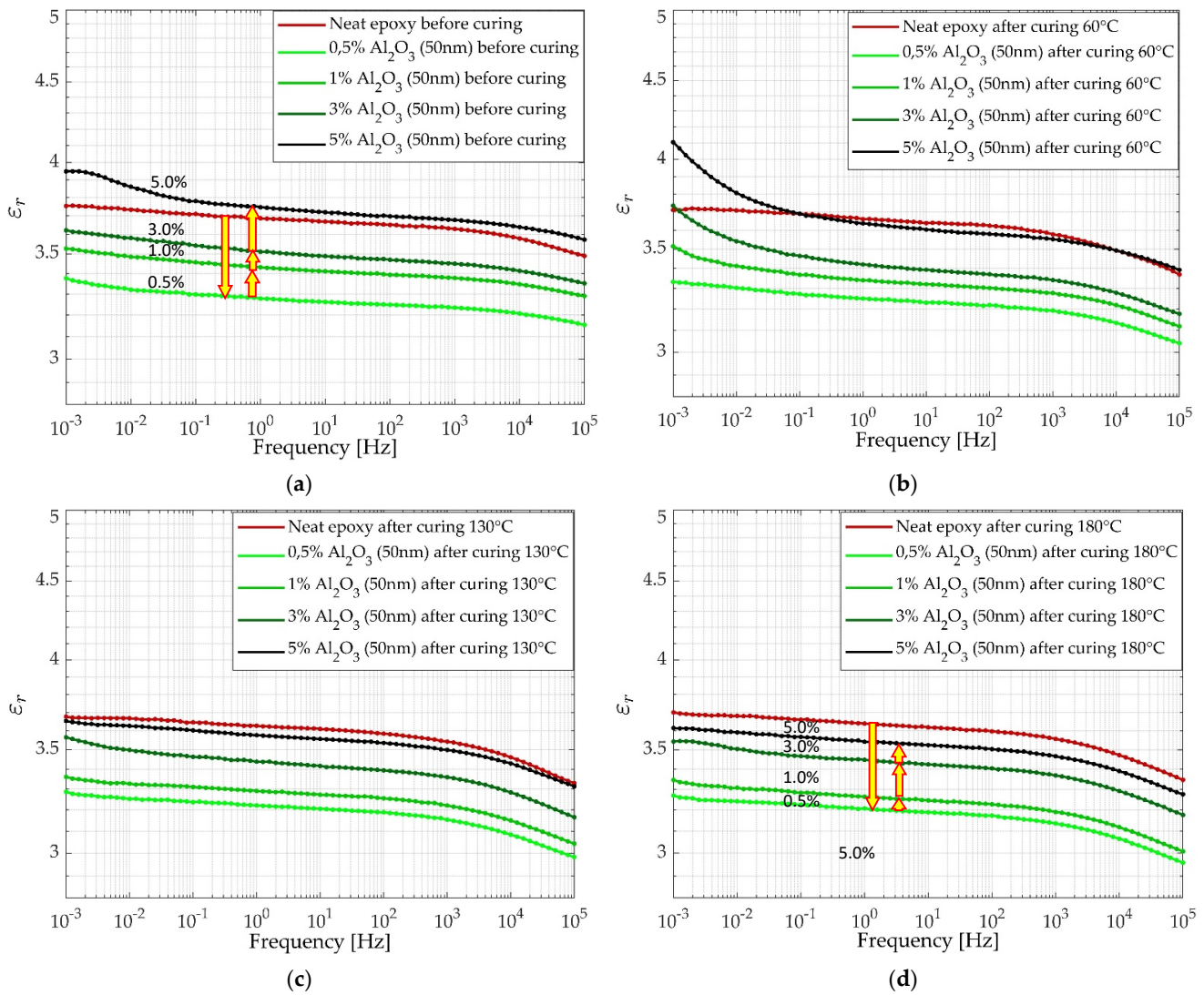


**Figure 4.** Broadband dielectric constant  $\epsilon_r(f)$  characteristics for samples with  $\text{Al}_2\text{O}_3$ , with particles of 50 nm: (a) new, before curing, (b) after thermal curing at 60 °C, (c) after thermal curing at 130 °C, (d) after thermal curing at 180 °C.

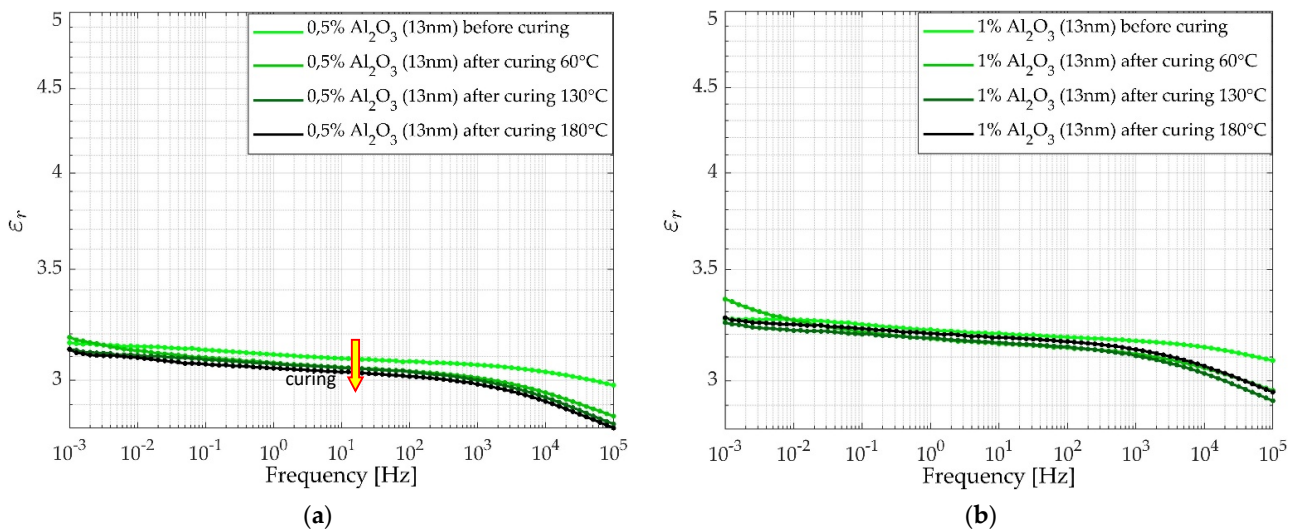


**Figure 5.** Cont.

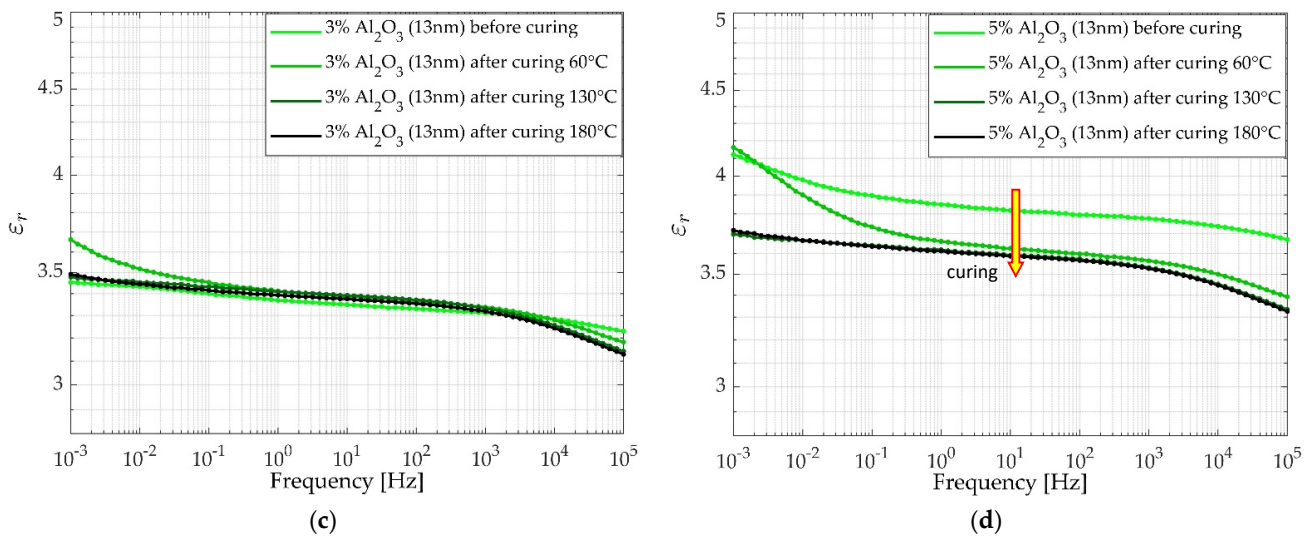


**Figure 5.** Broadband dielectric constant  $\epsilon_r(f)$  characteristics for samples with  $\text{Al}_2\text{O}_3$ , with particles of 13 nm and different wt% loadings: (a) 0.5%, (b) 1%, (c) 3%, (d) 5%.

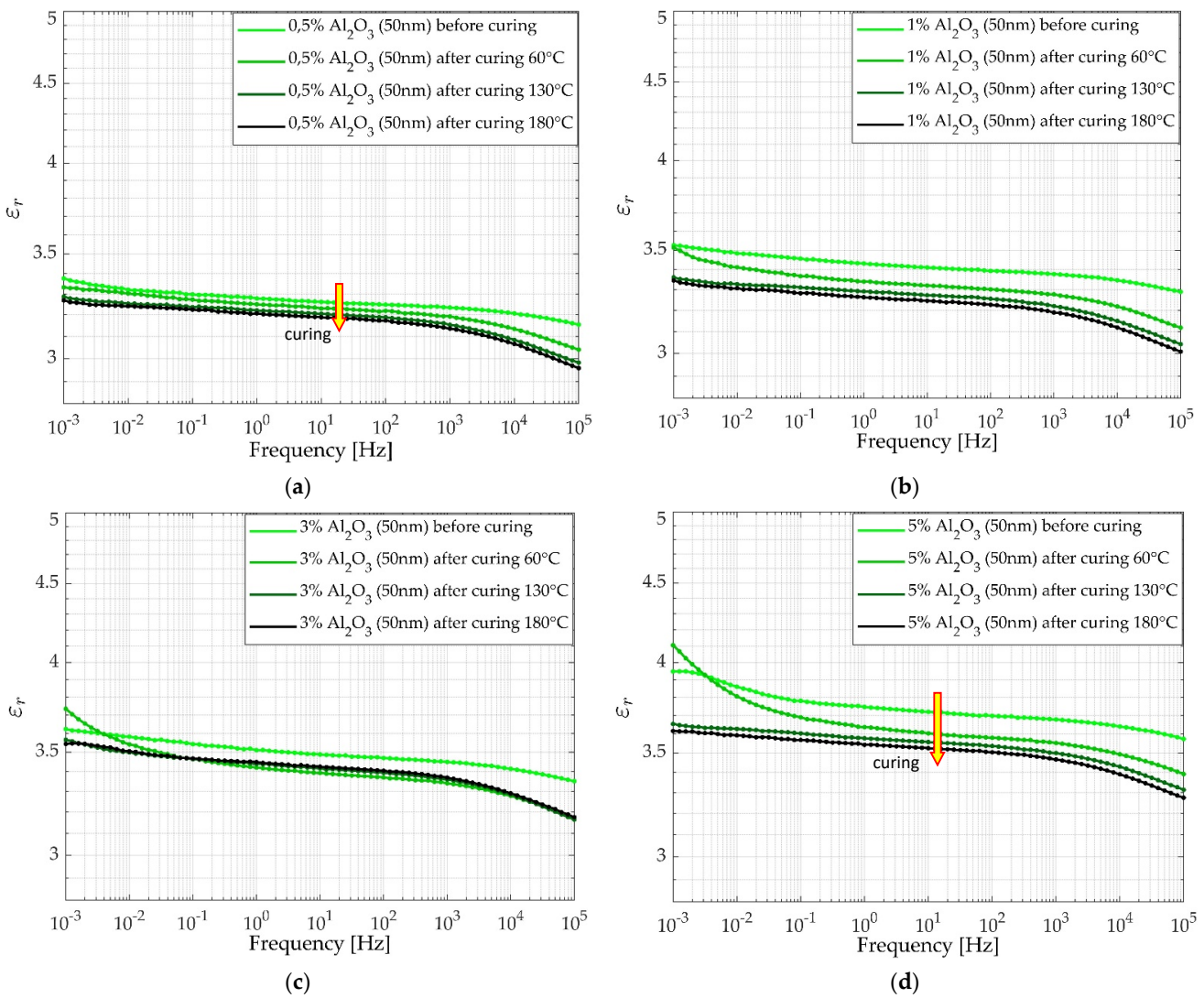


**Figure 6.** Broadband dielectric constant  $\epsilon_r(f)$  characteristics for samples with  $\text{Al}_2\text{O}_3$ , with particles of 50 nm and different wt% loadings: (a) 0.5%, (b) 1%, (c) 3%, (d) 5%.

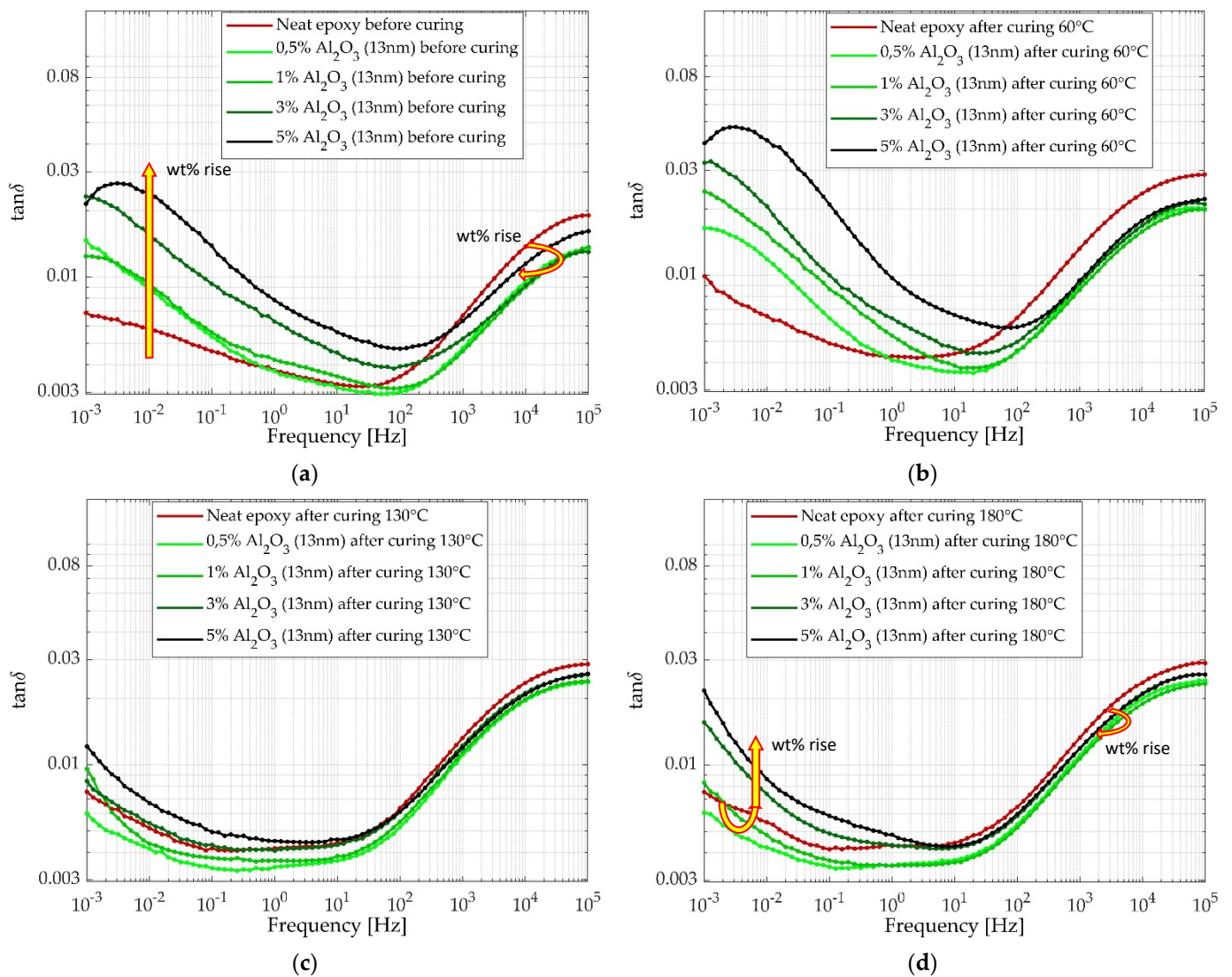


**Figure 7.** Broadband dielectric loss factor  $\tan\delta(f)$  characteristics for samples with  $\text{Al}_2\text{O}_3$ , with particles of 13 nm: (a) new, before curing, (b) after thermal curing at 60 °C, (c) after thermal curing at 130 °C, (d) after thermal curing at 180 °C.

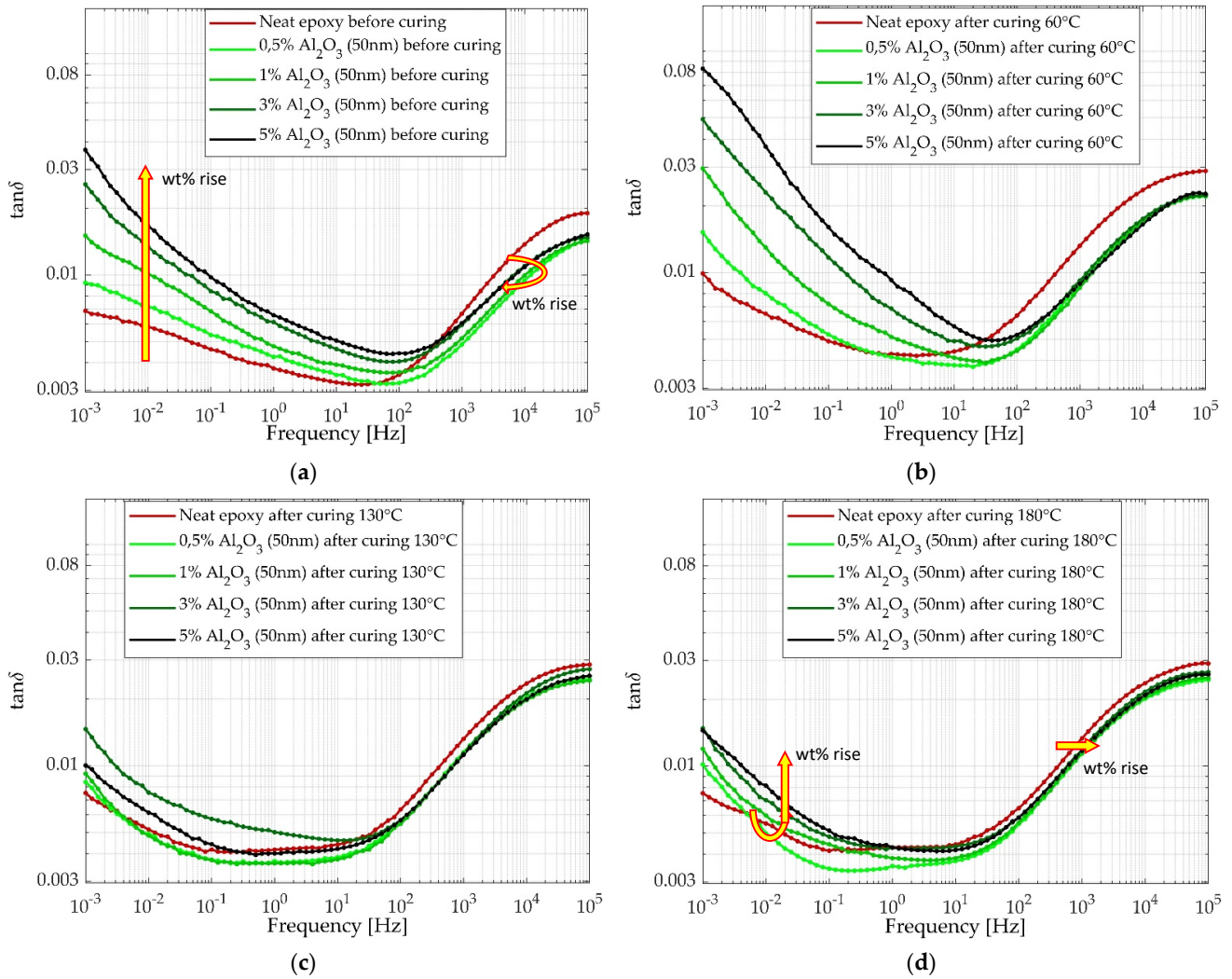


**Figure 8.** Broadband dielectric loss factor  $\tan\delta(f)$  characteristics for samples with Al<sub>2</sub>O<sub>3</sub>, with particles of 50 nm: (a) new, before curing, (b) after thermal curing at 60 °C, (c) after thermal curing at 130 °C, (d) after thermal curing at 180 °C.

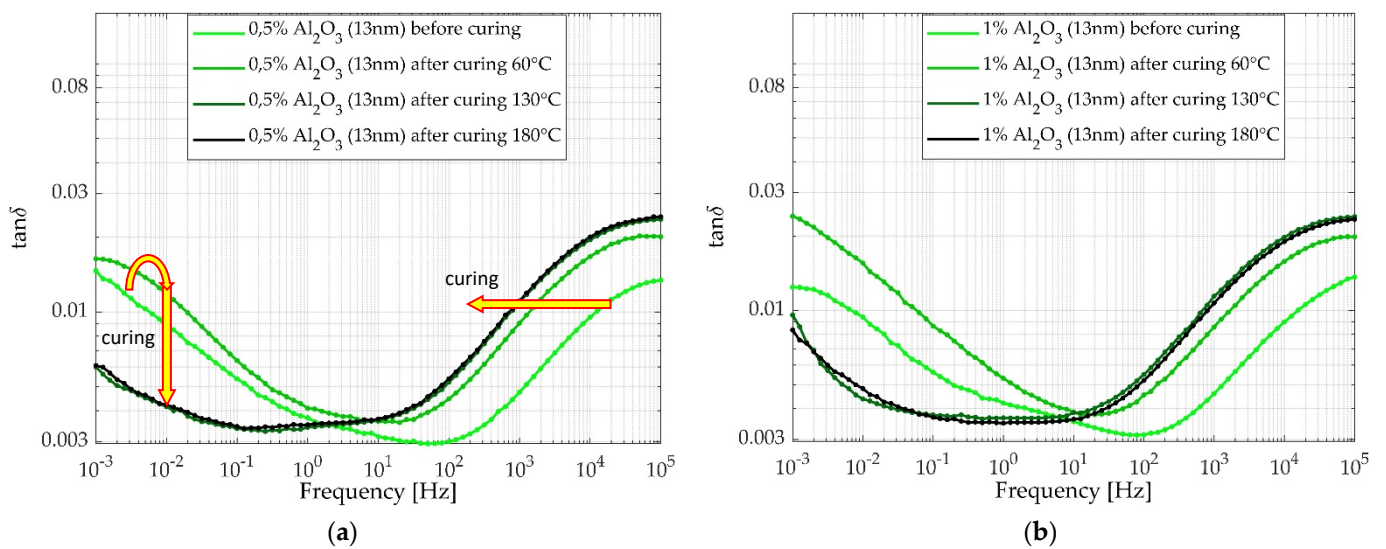


**Figure 9.** Cont.

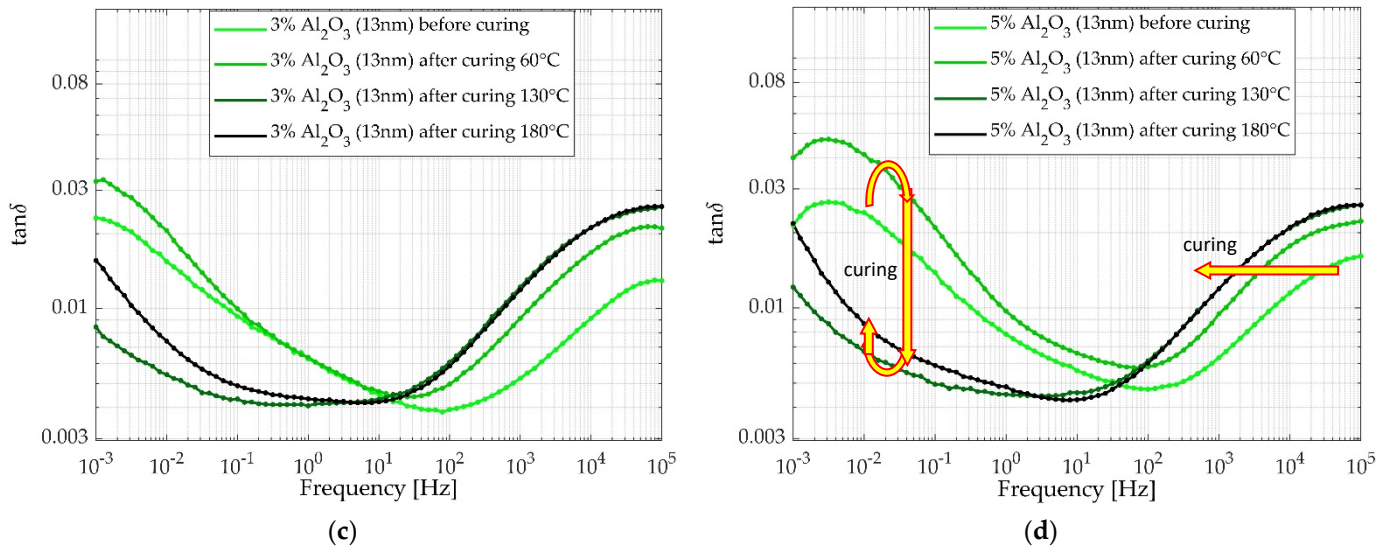


**Figure 9.** Broadband dielectric loss factor  $\tan\delta(f)$  characteristics for samples with  $\text{Al}_2\text{O}_3$ , with particles 13 nm and different wt% loadings: (a) 0.5%, (b) 1%, (c) 3%, (d) 5%.

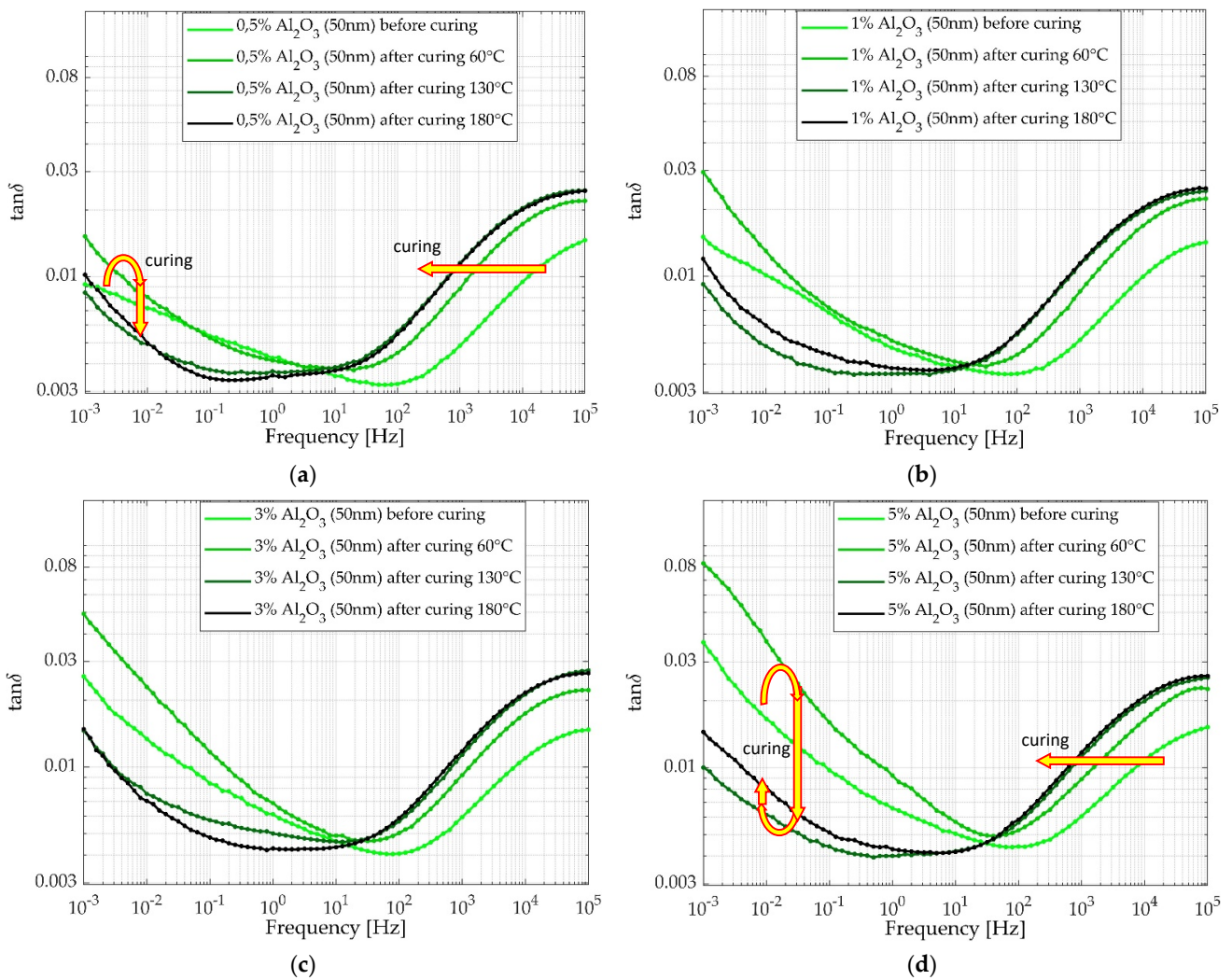


**Figure 10.** Broadband dielectric loss factor  $\tan\delta(f)$  characteristics for samples with  $\text{Al}_2\text{O}_3$ , with particles of 50 nm and different wt%: (a) 0.5%, (b) 1%, (c) 3%, (d) 5%.

#### 4. Discussion

In each of the analyzed cases, for epoxy resin samples without and with a nanofiller, the value of the dielectric constant  $\epsilon_r$  decreased with increasing frequency. The measurement results for neat resin samples without nanofiller (Figure 2a) indicate that the pre-curing of the virgin sample at 60 °C and subsequent curing and post-curing cycles at higher temperatures slightly lower the dielectric constant values over the entire range of the analyzed frequencies [46]. These changes are more pronounced for frequencies above 400 Hz. At the same time, broadband characteristics of the dielectric loss factor indicate that for gradually cured samples, its values for the range of higher frequencies (above 1 Hz) increase. There is also a visible shift of the transition band of high-frequency losses to the left, towards lower frequencies. Differences in the value of losses for frequencies below 1 Hz are not so significant. Curing effects are greatest after the first curing cycle at 60 °C and are almost negligible after subsequent cycles (both characteristics after curing at 130 °C and 180 °C are almost identical). Such effects result from thermally accelerated cross-linking processes of the epoxy matrix, which affect the lower availability and mobility of reactive groups. At this stage, the rate of curing is not determined by the kinetics of chemical reactions, but rather by the rate of diffusion, which decreases [58]. The peak of dielectric losses at higher observed frequencies is related to the  $\beta$ -relaxation process [59,60], which is linked to the mobility of polymer side chains [60,61]. The first cycle of epoxy resin curing (at 60 °C) shifts this peak to the left, which means that in the higher range of frequencies (for  $f > 1$  Hz), there is an increase in dielectric losses. Subsequent hardening cycles do not cause further significant changes in the characteristics of  $\tan\delta(f)$ . The results obtained for the neat resin are used as the basic reference for all other analyzed cases.

In the case of polymers, their dielectric parameters largely depend on the number of orientable dipoles present in the system and their ability to orient under the external electric field of a certain frequency. At lower frequencies, more dipoles can reorient themselves quickly enough in the epoxy resin structure, resulting in a higher dielectric constant. At a higher frequency, there will be fewer such dipoles, leading to a decrease in this quantity. For samples cured at 130 °C and 180 °C, the plots of the dielectric constant flatten below 1 Hz, indicating that further lowering the frequency only slightly increases the number of dipoles involved in the accumulation of electric charge. This effect occurs both in neat epoxy resin and nanocomposite samples [33,62,63].

The broadband characteristics obtained for the measurement results of resin samples modified with a different wt% content of nano-alumina allow us to determine noticeable changes in dielectric parameters caused by the presence of nanofiller. Figures 3–6 show the broadband characteristics of the dielectric constant. The use of nanofillers results in lower dielectric constant values than neat resin over the entire frequency range for any nanofiller content (0.5 wt% to 5.0 wt%), except for samples with 5.0 wt% before curing. The most significant is the reduction of the dielectric constant for the samples with 0.5 wt% of nanofiller (Figures 3 and 4). This effect occurs for both sizes of nanoparticles, but the decrease in the value for the  $\epsilon_r(f)$  characteristic is greater for the 13 nm nanofiller. The presence of nanofiller particles in the cross-linked long-chain molecular structure of epoxy resin causes the occurrence of two independent processes with an opposite effect on the phenomenon of accumulation of electric charges in the dielectric:

1. Reducing the ability of the base structure of the nanocomposite (epoxy resin polymer matrix) to accumulate charges [29,33];
2. The accumulation of additional charges caused by the presence of the interphase of nanoparticles and as a result of the occurrence of Maxwell–Wagner–Sillars polarization [64,65] in the two- or multi-phase structure of the nanocomposite.

The mechanism of decreasing the dielectric constant value of the nanocomposite is related to the reduction of the mobility of polymer chains in the presence of filler nanoparticles dispersed in the base polymer. As a result of the interaction of the polymer with the nanoparticle, on the surface of which the interfacial nano-layer is formed, a strong bond of polymer chains with the surface of the particle is formed [33,66]. If this

phenomenon affects all or most of the nanoparticles filling the polymer matrix, it can be assumed that the mobility of the polymer segments or chains interacting with nanoparticles will be partially blocked or limited to some extent [29]. These immobile polymer chains reduce polarization in the epoxy, thus leading to the reduction in the dielectric constant value. The effect is more significant for 13 nm nanoparticles for which the inter-particle distance is several times smaller than for nanoparticles with an average size of 50 nm (Table 1). As a result, there are over 50 times more of these smaller nanoparticles in the same volume of the nanocomposite compared to the second case. For wt% greater than 0.5%, the increasing content of nanofiller (for both sizes of Al<sub>2</sub>O<sub>3</sub> nanoparticles used in the research) causes a corresponding gradual increase in the dielectric constant value. Such effects have already been observed and described in other studies [25,29–31]. This phenomenon occurs most likely as a result of the decreasing intermolecular distance and the overlapping of interphases. Then, the properties of the composite are more influenced by the nanofiller itself and its permittivity [25,33].

The influence of the Al<sub>2</sub>O<sub>3</sub> nanoparticle size, the wt% value, and the curing temperature on the  $\epsilon_r(f)$  characteristics are noticeable in the results presented in Figure 11. For the nanocomposite before curing (Figure 11a), at 0.5 wt% of the nanofiller content, there is a greater decrease in the relative permittivity in the entire analyzed frequency range for nanoparticles of smaller size. The inverse effect of nanoparticle size on permittivity can be observed for ten times higher nanofiller content weight (5.0 wt%). A greater increase in permittivity then occurs also for Al<sub>2</sub>O<sub>3</sub> nanoparticles with a size of 13 nm. Gradual curing, at increasingly higher temperatures up to 180 °C (Figure 11b–d), affects both of these opposite effects, but more the effect of increasing the permittivity for the 5.0 wt% content of nanofillers. After curing, the  $\epsilon_r(f)$  characteristics for 5% of the content of 13 nm Al<sub>2</sub>O<sub>3</sub> particles are almost identical to those for neat epoxy resin, and for 50 nm Al<sub>2</sub>O<sub>3</sub> particles, it is slightly below the characteristics for neat resin.

The results of the described experiments show that the thermosetting of the epoxy structure (and thus, its stiffening), which is in strong interaction with the nanoparticles of the Al<sub>2</sub>O<sub>3</sub> filler, also reduces to some extent the additional charge accumulated as a result of the presence of nanoparticles in this structure. This means that the net permittivity of the nanocomposite is the result of mutual, complex interactions of the polymer base structure of the epoxy resin and the Al<sub>2</sub>O<sub>3</sub> nanoparticles dispersed in it.

The broadband characteristics of the epoxy-alumina nanocomposite dielectric loss factor (Figures 7–10 and 12), in which there is an effect of the Al<sub>2</sub>O<sub>3</sub> nanoparticle interphase, are related to the nanoparticle–epoxy matrix interaction and relaxation with extra polarization losses caused by additional polar groups [67]. The electrical conductivity of a nanocomposite is also the parameter that modified the dielectric loss factor, especially in the low-frequency region. It depends on the frequency, the relaxation time of the charge carriers, and the number of charge carriers available in the material. The addition of the Al<sub>2</sub>O<sub>3</sub> nanoparticles to the polymer matrix increases the charge carriers in the system, so an increase in the dielectric loss factor in the low-frequency range can be expected with an increase in the nanofiller content [31]. Higher wt% loading of nanofiller causes a visible increase in dielectric loss factor in the lower frequency range (below 10 Hz) of the new and the pre-cured nanocomposite (Figures 7 and 8). The losses in this frequency range are influenced also by mentioned interface polarization processes related to the presence of the nanofiller interphase. Thermosetting processes strongly affect the broadband characteristics of the dielectric loss factor. Curing the samples at the highest temperatures used in the experiment significantly reduces these losses for the low-frequency range (<100 Hz). This effect is noticeable for nanocomposite samples with both dimensions of the nanofiller particles (Figures 9 and 10), especially for the nanofiller content of 0.5 wt%.

In general, it can be stated that curing at gradually higher temperatures causes a decrease in the dielectric constant for all tested nanocomposite samples in the full range of analyzed frequencies (Figures 5 and 6). On the other hand, changes in the dielectric loss factor observed during the curing process of each of the tested samples are non-monotonic.

In the low-frequency range, in the successive stages of curing, there was an increase, then a decrease, and again an increase in dielectric loss values (Figures 9 and 10). Similar effect was observed for the imaginary component of the permittivity  $\epsilon''$  during isothermal curing of an epoxy-amine system at 140 °C [62]. These results indicate the complexity of the effects of the curing process in the nanocomposite structure, affecting the dielectric parameters.

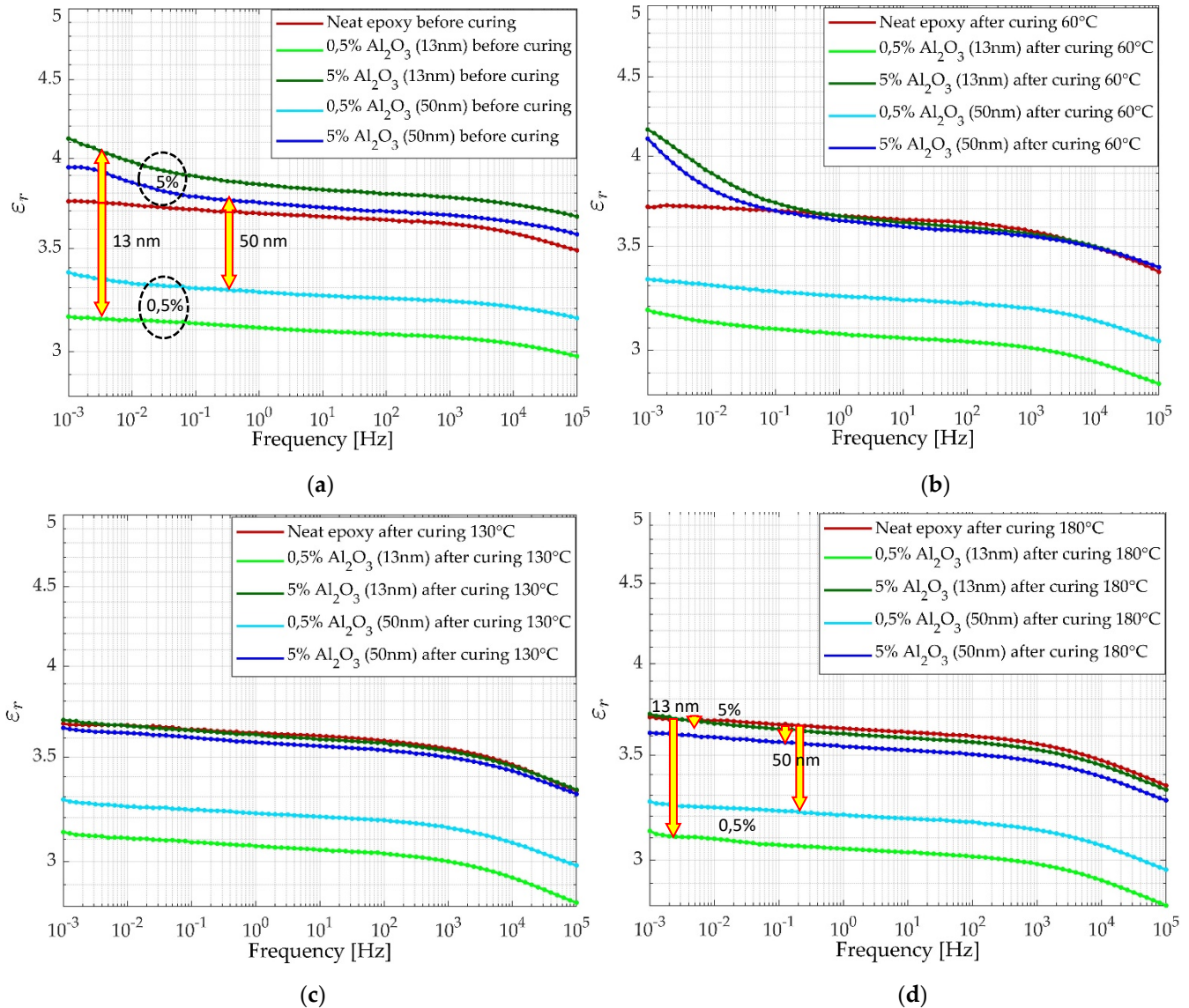


**Figure 11.** Selected curing temperature-dependent broadband characteristics of the dielectric constant for Al<sub>2</sub>O<sub>3</sub> nanoparticles with an average size of 13 nm and <50 nm, for two limit values of wt% used during the tests, 0.5% and 5.0%: (a) new, before curing, (b) after thermal curing at 60 °C, (c) after thermal curing at 130 °C, (d) after thermal curing at 180 °C.

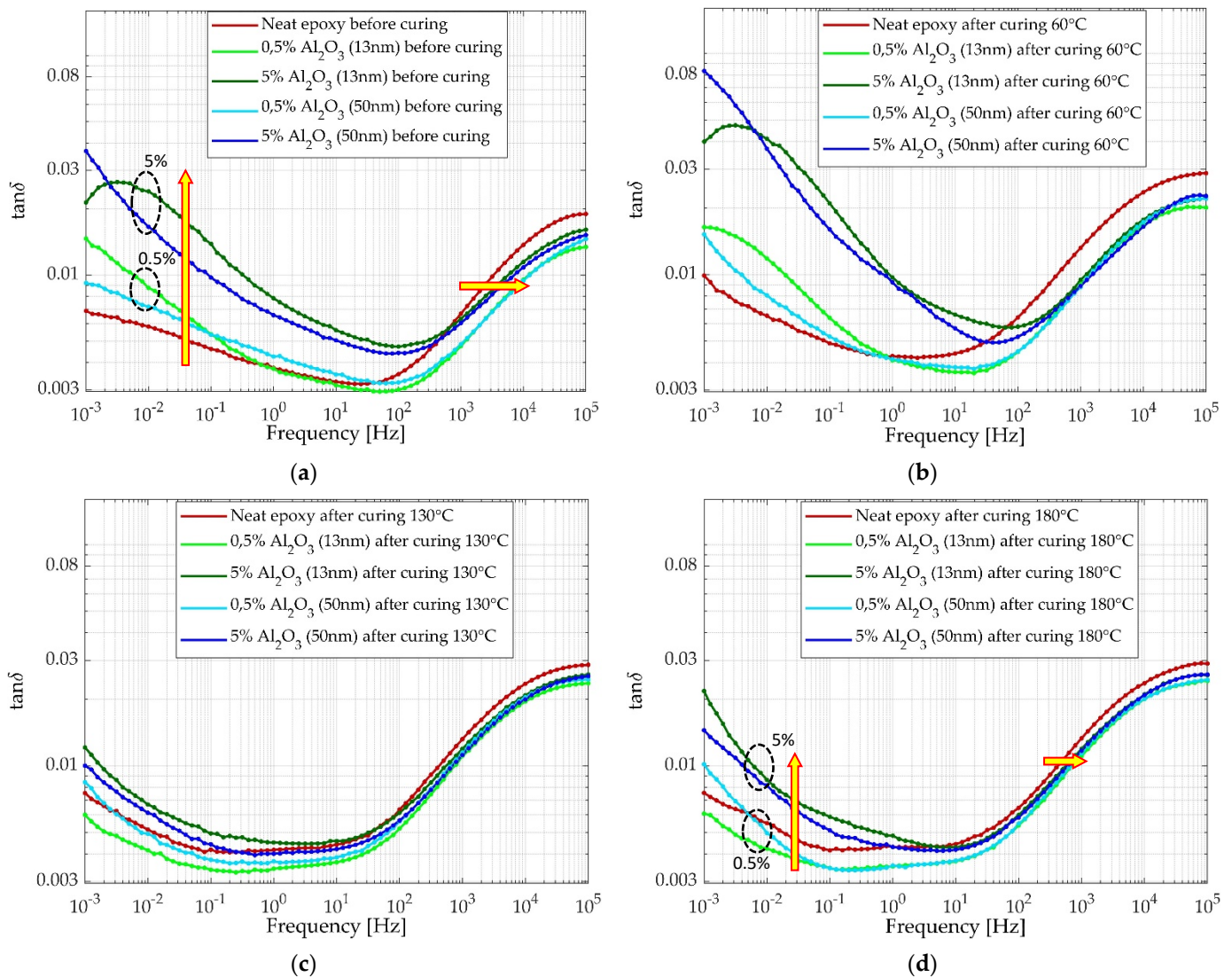


**Figure 12.** Selected curing temperature-dependent broadband characteristics of the dielectric losses for  $\text{Al}_2\text{O}_3$  nanoparticles with an average size of 13 nm and <50 nm, for two limit values of wt% used during the tests, 0.5% and 5.0%: (a) new, before curing, (b) after thermal curing at 60 °C, (c) after thermal curing at 130 °C, (d) after thermal curing at 180 °C.

## 5. Conclusions

(1) The laboratory experiment investigated the influence of gradual temperature curing on broadband characteristics of nanocomposite samples' dielectric properties (dielectric constant and dielectric loss factor). Changing the content of the  $\text{Al}_2\text{O}_3$  nanofiller in applied Class H epoxy resin modifies the characteristics of both analyzed dielectric parameters. The dielectric constant value of the nanocomposite decreases or increases in the full range of the tested frequencies, depending on the nanofiller content (wt%). Changing the content of  $\text{Al}_2\text{O}_3$  nanoparticles also modifies the dielectric loss factor characteristics, causing their shifts and increasing or decreasing in some frequency ranges. Such effects are the result of a complex interaction of nanoparticles with the base polymer chains. For all tested samples cured at 130 °C (and post-cured at 180 °C), the differences in the dielectric loss factor characteristics for frequencies greater than 100 Hz are low. For frequencies < 100 Hz, there are prominent differences in characteristics related to the nanoparticle size and the wt% loading.

(2) The conducted research shows that the analyzed parameters of the tested samples strongly depend on the stage of the applied curing procedure, i.e., on the degree of cross-

linking of the nanocomposite structure. The final broadband characteristics are the effect of the entire curing process, and this observation applies to dielectric constant as well as dielectric loss factor characteristics. The impact of curing on parameters is more significant for samples modified with nanofillers than for neat epoxy resin samples. Pre-curing at 60 °C is insufficient for the ultimate stabilization of broadband characteristics. The research results indicate that such stabilization is possible after curing and post-curing at higher temperatures (130 °C and 180 °C).

(3) The size of the Al<sub>2</sub>O<sub>3</sub> nanoparticles influences the changes in the characteristics of the dielectric parameters. The processes affecting the dielectric constant and the dielectric loss factor values are related to the presence of the nanoparticles. They are more effective for nanoparticles with a smaller size (i.e., with a larger specific surface area and a larger number of nanoparticles in the volume for a given wt%). This effect is visible in the test results for both lower (0.5 wt% and 1.0 wt%) and higher (3.0 wt% and 5.0 wt%) nanofiller content.

(4) At low nanofiller content (0.5 wt%) for both nanoparticle sizes, the samples after curing at 130 °C and 180 °C were characterized by noticeably lower dielectric constant and dielectric loss factor values than for neat resin, for the frequencies below 100 Hz. This effect can have application in the thermoset insulation systems design for electrical equipment operating with AC voltage (50 Hz/60 Hz).

**Author Contributions:** Conceptualization and methodology, P.Z.; formal analysis, A.D., P.B. and P.Z.; investigation and resources, A.D., P.B., M.K. and P.Z.; data curation, A.D., P.B. and P.Z.; writing—original draft preparation and revision, A.D., P.B. and P.Z.; visualization, A.D., P.B. and P.Z.; supervision and project administration, P.Z. All authors have read and agreed to the published version of the manuscript.

**Funding:** The research was financed by a subsidy of the Polish Minister of Education and Science for AGH University of Science and Technology, Krakow, Poland.

**Institutional Review Board Statement:** Not applicable.

**Data Availability Statement:** Not applicable.

**Conflicts of Interest:** The authors declare no conflict of interest.

## References

1. Nelson, J.K. *Dielectric Polymer Nanocomposites*; Springer: New York, NY, USA, 2010. [CrossRef]
2. Pleșa, I.; Noțingher, P.V.; Schlögl, S.; Sumereder, C.; Muhr, M. Properties of polymer composites used in high-voltage applications. *Polymers* **2016**, *8*, 173. [CrossRef] [PubMed]
3. Shao-Long, Z.; Zhi-Min, D.; Wen-Ying, Z.; Hui-Wu, C. Past and future on nanodielectrics. *IET Nanodielectr.* **2018**, *1*, 41–47. [CrossRef]
4. Hassan, Y.A.; Hu, H. Current status of polymer nanocomposite dielectrics for high-temperature applications. *Compos. Part A Appl. Sci. Manuf.* **2020**, *138*, 106064. [CrossRef]
5. Guastavino, F.; Ratto, A.; Torello, E.; Biondi, G. Aging tests on nanostructured enamels for winding wire insulation. *IEEE Trans. Industr. Electron.* **2014**, *61*, 5550–5557. [CrossRef]
6. Hornak, J.; Mentlík, V.; Trnka, P.; Šutta, P. Synthesis and diagnostics of nanostructured micaless microcomposite as a prospective insulation material for rotating machines. *Appl. Sci.* **2019**, *9*, 2926. [CrossRef]
7. Zhou, Y.; Peng, S.; Hu, J.; He, J. Polymeric insulation materials for HVDC cables: Development, challenges and future perspective. *IEEE Trans. Dielectr. Electr. Insul.* **2017**, *24*, 1308–1318. [CrossRef]
8. Guo, M.; Fréchette, M.; David, É.; Demarquette, N.R.; Daigle, J.-C. Polyethylene/polyhedral oligomeric silsesquioxanes composites: Electrical insulation for high voltage power cables. *IEEE Trans. Dielectr. Electr. Insul.* **2017**, *24*, 798–807. [CrossRef]
9. Mansour, D.-E.A.; Elsaheed, A.M.; Izzularab, M.A. The role of interfacial zone in dielectric properties of transformer oil-based nanofluids. *IEEE Trans. Dielectr. Electr. Insul.* **2016**, *23*, 3364–3372. [CrossRef]
10. Primo, V.A.; García, B.; Burgos, J.C.; Pérez-Rosa, D. Investigation of the lightning impulse breakdown voltage of mineral oil based Fe<sub>3</sub>O<sub>4</sub> nanofluids. *Coatings* **2019**, *9*, 799. [CrossRef]
11. Wang, J.; Xie, Y.; Liu, J.; Zhang, Z.; Zhuang, Q.; Kong, J. Improved energy storage performance of linear dielectric polymer nanodielectrics with polydopamine coated BN nanosheets. *Polymers* **2018**, *10*, 1349. [CrossRef]

12. O'Connor, K.A.; Kutz, R.B.; Miranda, M.; Curry, R.D. Design and testing of a compact 40 kV capacitor based on nanodielectric composites. In Proceedings of the 2019 IEEE Pulsed Power & Plasma Science (PPPS), Orlando, FL, USA, 23–29 June 2019; pp. 1–4. [[CrossRef](#)]
13. Chi, X.; Liu, W.; Li, S.; Zhang, X. The effect of humidity on dielectric properties of PP-based nano-dielectric. *Materials* **2019**, *12*, 1378. [[CrossRef](#)] [[PubMed](#)]
14. Xiao, M.; Du, B.X. Review of high thermal conductivity polymer dielectrics for electrical insulation. *High Volt.* **2016**, *1*, 34–42. [[CrossRef](#)]
15. Zhang, D.-L.; Zha, J.-W.; Li, C.-Q.; Li, W.-K.; Wang, S.-J.; Wen, Y.; Dang, Z.-M. High thermal conductivity and excellent electrical insulation performance in double-percolated three-phase polymer nanocomposites. *Compos. Sci. Technol.* **2017**, *144*, 36–42. [[CrossRef](#)]
16. Rybak, A.; Jarosinski, L.; Gaska, K.; Kapusta, C. Graphene nanoplatelet-silica hybrid epoxy composites as electrical insulation with enhanced thermal conductivity. *Polym. Compos.* **2018**, *39*, E1682–E1691. [[CrossRef](#)]
17. Rybak, A. Processing influence on thermal conductivity of polymer nanocomposites. In *Processing of the Polymer Nanocomposites*; Kenig, S., Ed.; Carl Hanser Verlag GmbH & Co.: Munich, Germany, 2019; pp. 463–487. [[CrossRef](#)]
18. Lewis, T.J. Nanometric dielectrics. *IEEE Trans. Dielectr. Electr. Insul.* **1994**, *1*, 812–825. [[CrossRef](#)]
19. Couderc, H.; Fréchette, M.F.; Savoie, S.; David, E. Nanofiller effect during post-heat treatment of micro-loaded epoxy. In Proceedings of the 2010 Annual Report Conference on Electrical Insulation and Dielectric Phenomena (CEIDP), West Lafayette, IN, USA, 17–20 October 2010; pp. 1–4. [[CrossRef](#)]
20. Lewis, T.J. Interfaces are the dominant feature of dielectrics at the nanometric level. *IEEE Trans. Dielectr. Electr. Insul.* **2004**, *11*, 739–753. [[CrossRef](#)]
21. Fréchette, M.F.; Preda, I.; Castellon, J.; Krivda, A.; Veillette, R.; Trudeau, M.; David, E. Polymer composites with a large nanofiller content: A case study involving epoxy. *IEEE Trans. Dielectr. Electr. Insul.* **2014**, *21*, 434–443. [[CrossRef](#)]
22. Adnan, M.M.; Tveten, E.G.; Glaum, J.; Ese, M.-H.G.; Hvidsten, S.; Glomm, W.; Einarsrud, M.-A. Epoxy-based nanocomposites for high-voltage insulation: A review. *Adv. Electron. Mater.* **2018**, *5*, 1800505. [[CrossRef](#)]
23. Kuruvilla, S.P.; Renukappa, N.M.; Rajan, J.S. Development of epoxy with nano and micro fillers for core insulation of composite insulators. In Proceedings of the 2019 International Conference on High Voltage Engineering and Technology (ICHVET), Hyderabad, India, 7–8 February 2019; pp. 1–5. [[CrossRef](#)]
24. Li, Z.; Okamoto, K.; Ohki, Y.; Tanaka, T. The role of nano and micro particles on partial discharge and breakdown strength in epoxy composites. *IEEE Trans. Dielectr. Electr. Insul.* **2011**, *18*, 675–681. [[CrossRef](#)]
25. Parmar, A.K.; Patel, R.R. Dielectric properties of alumina based epoxy composites for electrical insulation. In Proceedings of the 2018 2nd International Conference on Electronics, Materials Engineering & Nano-Technology (IEMENTech), Kolkata, India, 4–5 May 2018; pp. 1–4. [[CrossRef](#)]
26. Castellon, J.; Nguyen, H.N.; Agnel, S.; Tourelle, A.; Fréchette, M.F.; Savoie, S.; Krivda, A.; Schmidt, L.E. Electrical properties analysis of micro and nano composite epoxy resin materials. *IEEE Trans. Dielectr. Electr. Insul.* **2011**, *18*, 651–658. [[CrossRef](#)]
27. Yanashima, R.; Hirai, N.; Ohki, Y. Effects of addition of MgO fillers with various sizes and co-addition of nano-sized SiO<sub>2</sub> fillers on the dielectric properties of epoxy resin. In Proceedings of the 2017 International Symposium on Electrical Insulating Materials (ISEIM), Toyohashi, Japan, 11–15 September 2017; pp. 650–653. [[CrossRef](#)]
28. Faiza Khattak, A.; Alahamdi, A.A.; Iqbal, M.B. Degradation performance investigation of hydrothermally stressed epoxy micro and nanocomposites for high voltage insulation. *Polymers* **2022**, *14*, 1094. [[CrossRef](#)]
29. Singha, S.; Thomas, M.J. Permittivity and tan delta characteristics of epoxy nanocomposites in the frequency range of 1 MHz-1 GHz. *IEEE Trans. Dielectr. Electr. Insul.* **2008**, *15*, 2–11. [[CrossRef](#)]
30. Shi, H.; Gao, N.; Jun, H.; Zhang, G.; Peng, Z. Investigation of the effects of nano-filler on dielectric properties of epoxy based composites. In Proceedings of the 2009 IEEE 9th International Conference on the Properties and Applications of Dielectric Materials, Harbin, China, 19–23 July 2009; pp. 804–807. [[CrossRef](#)]
31. Singha, S.; Thomas, M.J. Dielectric properties of epoxy-Al<sub>2</sub>O<sub>3</sub> nanocomposite system for packaging applications. *IEEE Trans. Compon. Packag. Technol.* **2010**, *33*, 373–385. [[CrossRef](#)]
32. Jiang, P.; Yu, J.; Huang, X. Influence of interface chemistry on dielectric properties of epoxy/alumina nanocomposites. In Proceedings of the 2015 IEEE Electrical Insulation Conference (EIC), Seattle, WA, USA, 7–10 June 2015; pp. 621–624. [[CrossRef](#)]
33. Lyu, X.; Wang, H.; Guo, Z.; Peng, Z. Dielectric properties of epoxy-Al<sub>2</sub>O<sub>3</sub> nanocomposites. In Proceedings of the 2016 IEEE International Conference on Dielectrics, Montpellier, France, 3–7 July 2016; pp. 1081–1084. [[CrossRef](#)]
34. Samuel, J.G.C.; Lafon-Placette, S.; Fu, M.; Howard, P.J.; Perrot, F. Epoxy-alumina nanocomposites: Advanced materials for high-voltage insulation? In Proceedings of the 2012 Annual Report Conference on Electrical Insulation and Dielectric Phenomena (CEIDP), Montreal, QC, Canada, 14–17 October 2012; pp. 573–576. [[CrossRef](#)]
35. Kozako, M.; Yamano, S.; Kido, R.; Ohki, Y.; Kohtoh, M.; Okabe, S.; Tanaka, T. Preparation and preliminary characteristic evaluation of epoxy/alumina nanocomposites. In Proceedings of the 2005 International Symposium on Electrical Insulating Materials, (ISEIM 2005), Kitakyushu, Japan, 5–9 June 2005; Volume 1, pp. 231–234. [[CrossRef](#)]
36. Peihong, Z.; Lingyun, G.; Gang, L.; Qingquan, L. Study on dielectric characteristics of nano-Al<sub>2</sub>O<sub>3</sub> composite polyimide film. In Proceedings of the 2006 IEEE 8th International Conference on Properties & Applications of Dielectric Materials, Bali, Indonesia, 26–30 June 2006; pp. 759–762. [[CrossRef](#)]
37. Li, Z.; Okamoto, K.; Ohki, Y.; Tanaka, T. Effects of nano-filler addition on partial discharge resistance and dielectric breakdown strength of micro-Al<sub>2</sub>O<sub>3</sub> epoxy composite. *IEEE Trans. Dielectr. Electr. Insul.* **2010**, *17*, 653–661. [[CrossRef](#)]

38. Yu, S.; Yu, X.; Lian, Z.; Wang, S.; Nie, Y.; Li, S. Effect of nano- $\text{Al}_2\text{O}_3$  and micro- $\text{Al}(\text{OH})_3$  co-doping on epoxy resin properties. In Proceedings of the 2020 IEEE International Conference on High Voltage Engineering and Application (ICHVE), Beijing, China, 6–10 September 2020; pp. 1–4. [\[CrossRef\]](#)
39. Dađa, A.; Błaut, P. Research on dielectric parameters of epoxy resin based nanocomposites using the impedance spectroscopy method. *Prz. Elektrotech.* **2021**, *97*, 234–237. [\[CrossRef\]](#)
40. Elantas Europe. *EpoxyLite 235SG Trickle Impregnating Resin*; Product information; Elantas Europe: Hamburg, Germany, 2007.
41. May, C.A. *Epoxy Resins: Chemistry and Technology*, 2nd ed.; Marcel Dekker Inc.: New York, NY, USA, 1988.
42. Ellis, B. *Chemistry and Technology of Epoxy Resins*; Springer Science+Business Media: Dordrecht, The Netherlands, 1993.
43. Alhabill, F.N.; Ayoob, R.; Andritsch, T.; Vaughan, A.S. Effect of resin/hardener stoichiometry on electrical behavior of epoxy networks. *IEEE Trans. Dielectr. Electr. Insul.* **2017**, *24*, 3739–3749. [\[CrossRef\]](#)
44. Saeedi, I.A.; Chalashkanov, N.; Dissado, L.A.; Vaughan, A.S.; Andritsch, T. The nature of the gamma dielectric relaxation in diglycidyl ether Bisphenol-A (DGEBA) based epoxies. *Polymer* **2022**, *249*, 124861. [\[CrossRef\]](#)
45. Li, J.; Guo, P.; Kong, X.; Wang, Y.; Li, F.; Du, B. Curing degree dependence of dielectric properties of bisphenol-A-based epoxy resin cured with methyl hexahydrophthalic anhydride. *IEEE Trans. Dielectr. Electr. Insul.* **2022**, *29*, 2072–2079. [\[CrossRef\]](#)
46. Li, J.; Aung, H.H.; Du, B. Curing regime-modulating insulation performance of anhydride-cured epoxy resin: A review. *Molecules* **2023**, *28*, 547. [\[CrossRef\]](#)
47. Sigma-Aldrich Corp. *Aluminum Oxide Nanopowder, 13 nm Primary Particle Size-Product Specification*; Sigma-Aldrich Corp.: St. Louis, MS, USA, 2022.
48. Sigma-Aldrich Corp. *Aluminum Oxide Nanopowder, <50 nm Particle Size (TEM)-Product Specification*; Sigma-Aldrich Corp.: St. Louis, MS, USA, 2022.
49. Preetha, P.; Thomas, M.J. AC breakdown characteristics of epoxy nanocomposites. *IEEE Trans. Dielectr. Electr. Insul.* **2011**, *18*, 1526–1534. [\[CrossRef\]](#)
50. Tanaka, T.; Kozako, M.; Fuse, N.; Ohki, Y. Proposal of a multi-core model for polymer nanocomposite dielectrics. *IEEE Trans. Dielectr. Electr. Insul.* **2005**, *12*, 669–681. [\[CrossRef\]](#)
51. Kremer, F.; Schönhals, A. *Broadband Dielectric Spectroscopy*; Springer: Berlin, Germany, 2003.
52. Barsoukov, E.; Macdonald, J.R. *Impedance Spectroscopy. Theory, Experiment, and Applications*, 2nd ed.; John Wiley & Sons, Inc.: Hoboken, NJ, USA, 2005.
53. Solartron Analytical. *1260A Impedance/Gain-Phase Analyzer; Operating Manual*; Solartron Analytical: Wokingham, UK, 1996.
54. Solartron Analytical. *1296A Dielectric Interface; User guide*; Solartron Analytical: Wokingham, UK, 2003.
55. IEC 62631-2-1:2018; Dielectric and Resistive Properties of Solid Insulating Materials-Part 2-1: Relative Permittivity and Dissipation Factor-Technical Frequencies (0.1 Hz–10 MHz)-AC Methods. IEC: Geneva, Switzerland, 2018.
56. ASTM D150-18; Standard Test Methods for AC Loss Characteristics and Permittivity (Dielectric Constant) of Solid Electrical Insulation. ASTM: West Conshohocken, PA, USA, 2018.
57. IEC 60085:2007; Electrical Insulation-Thermal Evaluation and Designation. IEC: Geneva, Switzerland, 2007.
58. Jungang, G.; Shigang, S.; Yangfang, L.; Deling, L. Curing kinetics and thermal property characterization of bisphenol-F epoxy resin and DDS system. *Int. J. Polym. Mater. Polym. Biomater.* **2004**, *53*, 341–354. [\[CrossRef\]](#)
59. Saeedi, I.A.; Vaughan, A.S.; Andritsch, T.; Virtanen, S. The effect of curing conditions on the electrical properties of an epoxy resin. In Proceedings of the 2016 IEEE Conference on Electrical Insulation and Dielectric Phenomena (CEIDP), Toronto, ON, Canada, 16–19 October 2016; pp. 461–464. [\[CrossRef\]](#)
60. Preda, I.; Couderc, H.; Fréchette, M.; Savoie, S.; Gao, F.; Nigmatullin, R.; Thompson, S.; Castellon, J. Dielectric response of various partially cured epoxy nanocomposites. In Proceedings of the 2011 Annual Report Conference on Electrical Insulation and Dielectric Phenomena (CEIDP), Cancun, Mexico, 16–19 October 2011; pp. 660–663. [\[CrossRef\]](#)
61. Kochetov, R.; Andritsch, T.; Morshuis, P.H.F.; Smit, J.J. Anomalous behaviour of the dielectric spectroscopy response of nanocomposites. *IEEE Trans. Dielectr. Electr. Insul.* **2012**, *19*, 107–117. [\[CrossRef\]](#)
62. Eloundou, J.P. Dipolar relaxations in an epoxy-amine system. *Eur. Polym. J.* **2002**, *38*, 431–438. [\[CrossRef\]](#)
63. Livi, A.; Levita, V.; Rolla, P.A. Dielectric behavior at microwave frequencies of an epoxy resin during crosslinking. *J. Appl. Polymer. Sci.* **1993**, *50*, 1583–1590. [\[CrossRef\]](#)
64. Martinez-Vega, J. *Dielectric Materials for Electrical Engineering*; Wiley-ISTE: London, UK, 2013.
65. Samet, M.; Levchenko, V.; Boiteux, G.; Seytre, G.; Kallel, A.; Serghei, A. Electrode polarization vs. Maxwell-Wagner-Sillars interfacial polarization in dielectric spectra of materials: Characteristic frequencies and scaling laws. *J. Chem. Phys.* **2015**, *142*, 194703. [\[CrossRef\]](#) [\[PubMed\]](#)
66. Tsagaropoulos, G.; Eisenberg, A. Dynamic mechanical study of the factors affecting the two glass transition behavior of filled polymers. Similarities and differences with random ionomers. *Macromolecules* **1995**, *28*, 6067–6077. [\[CrossRef\]](#)
67. Zheng, Y.; Zhang, J.X.; Li, Q.; Chen, W.; Zhang, X. The influence of high content nano- $\text{Al}_2\text{O}_3$  on the properties of epoxy resin composites. *Polym. Plast. Technol. Eng.* **2009**, *48*, 384–388. [\[CrossRef\]](#)

**Disclaimer/Publisher’s Note:** The statements, opinions and data contained in all publications are solely those of the individual author(s) and contributor(s) and not of MDPI and/or the editor(s). MDPI and/or the editor(s) disclaim responsibility for any injury to people or property resulting from any ideas, methods, instructions or products referred to in the content.